Available online at www.sciencedirect.com

ScienceDirect

Journal of the European Ceramic Society 35 (2015) 2083–2089

www.elsevier.com/locate/jeurceramsoc

Electrophoretic deposition of (Zn, Nb)SnO_2-films varistor superficially modified with Cr^{3+}

Glauco Meireles Mascarenhas Morandi Lustosa [a,*], João Paulo de Campos da Costa [b], Leinig Antônio Perazolli [a], Biljana D. Stojanovic [c], Maria Aparecida Zaghete [a]

[a] *Laboratório Interdisciplinar de Eletroquímica e Cerâmica (LIEC), Instituto de Química, UNESP, Araraquara, SP, Brazil*
[b] *Centro Universitário de Araraquara (UNIARA), Araraquara, SP, Brazil*
[c] *Institute for Multidisciplinary Research, University of Belgrade, Belgrade, Serbia*

Received 7 November 2014; received in revised form 15 January 2015; accepted 20 January 2015
Available online 4 February 2015

Abstract

Recently, there has been an important rise in the research and development aimed to improve the properties of SnO_2-based varistors. Meanwhile, due to fact that ZnO-based varistors possess better electrical properties compared to SnO_2-based varistors, it is shown that it is needful to add additives to improve their properties. In our study, the SnO_2-powder was prepared by the chemical route (Pechini method) with addition of ZnO (1 mol%) and Nb_2O_5 (0.05 mol%). Films were obtained by the electrophoretic deposition of SnO_2-based powder, following by microwave oven sintering. Cr^{3+} was deposited by EPD on the films surface and thermal treatment was carried out in a microwave oven. After electrical characterization the films showed nonlinear coefficient over 10, breakdown voltage around 60 V, low leakage current ($\approx 10^{-6}$ A) and resistance over 200 kΩ cm. This indicates the efficiency of the used techniques to prepare varistor films with improved electrical properties after Cr^{3+} diffusion.

Keywords: SnO_2 varistor; Pechini; Electrophoretic deposition; Microwave sintering; Cr^{3+} diffusion

1. Introduction

Since the discovery of ZnO varistors by Matsuoka,[1] diverse arrays of researchers have sought to obtain varistors for use in electronic devices and appliances. The varistors, polycrystalline electronic ceramics with variable electrical resistance, are technologically important due to non-ohmic electric characteristics between the current and voltage, i.e., a high resistance during normal system operation (acting as an isolator) and a low resistance during overvoltage (acting as a conductor). The nonlinear properties of the ceramic are found to occur in the region of the grain boundaries of the material. Varistors could be used in electronic equipment as a protective device against overload voltage or in the energy distribution network against electric discharges.[2–4] The application of a ceramic varistor is related to the type and amount of effective barriers, which can be controlled during the processing step of the material (method of synthesis, types and amounts of additives, sintering, etc.).[2,5–8]

Combining the results of the ongoing research in SnO_2 ceramic varistors,[5,9–12] there is the possibility to obtaining SnO_2-films with varistor characteristics for the breakdown voltage system. According to the literature, additives that are introduced into the SnO_2-system are responsible for structural defects in the crystalline network such as oxygen vacancies, tin vacancies, which promote sintering densification and the addition of excess electrons that promotes conductivity in the grain.[12–15] The addition of the additives are responsible for creation of defects electron acceptors, and these defects may be in the grain boundary in order to improve the varistors characteristics, as can be seen in the equations:

$$ZnO \xrightarrow{SnO_2} Zn''_{Sn} + V_O^{\bullet\bullet} + O_O^X \quad (1)$$

* Corresponding author at: Instituto de Química, Universidade Estadual Paulista (UNESP), R. Prof. Francisco Degni, 55, Bairro Quitandinha, CEP 14800-060, Araraquara, SP, Brazil.
Tel.: +55 16 3301 9727/3332 7074/98233 6255.
E-mail address: glauco.morandi@gmail.com (G.M.M.M. Lustosa).

http://dx.doi.org/10.1016/j.jeurceramsoc.2015.01.022
0955-2219/

$$2Nb_2O_5 \xrightarrow{SnO_2} 4Nb_{Sn}^{\bullet\bullet} + V_{Sn}'' + 100_O^X \quad (2)$$

The presence of oxygen vacancies increases electron mobility, which in turn leads to an increase in the electronic conductivity in the grain. The created defects also cause an increase in the potential barrier layer, resulting in an increased resistivity in the grain boundary region. The addition of Cr_2O_3 is responsible for improvement of the nonlinear coefficient by influencing the characteristics of the potential barrier formed on the grain boundary.[6,11,15–17]

Filho et al.[18] suggested that the addition of chromium modifies the electronic states of the grain boundary region, increasing oxygen defects in the region (Eq. (3)) and resulting in more resistive samples and higher values of nonlinear coefficient. It was also noticed that the addition of Cr_2O_3 in the ceramic matrix modified the microstructure of SnO_2 resulting in a decrease in grain size due to formation of the secondary phase.[17–19] Aguilar-Martínez studied the influence of chromium on microstructure of SnO_2 and found that the addition of small amount did not lead to evident changes in the crystal lattice and to appearance of secondary phases. Meanwhile, due to the small concentration of Cr the presence of secondary phases cannot be detected by XRD.[20]

$$Cr_2O_3 \xrightarrow{SnO_2} 2Cr_{sn}' + 2V_O^{\bullet\bullet} + 3O_O^X \quad (3)$$

Previous studies of SnO_2-based varistor, reported by Cássia-Santos,[21] proposed that the Cr^{3+} ions added in ceramic matrix segregates in grain boundary region when used the heat treatment in conventional oven, promoting an increase in the values of resistivity and coefficient of non-linearity of the varistor system.

The methodology employed by the authors allows obtaining a solid solution without formation of secondary phases, and thus the ceramic powder possesses homogeneous composition and nanometric grains size. The addition of chromium is previously studied due to its important influence onto the varistor properties (properties of the grain boundary region). Therefore, in our study Cr^{3+} was added in the system by deposition on the film surface by EPD technique combined by heat treatment in a microwave oven. Thereafter, the influence of this additive on the non-ohmic properties of SnO_2-based system was investigated due to modification of grain boundary region. The aim was to promote Cr^{3+} diffusion in grain boundary region in order to avoid the effect of SnO_2 evaporation by reducing the sintering time used to segregate the Cr^{3+} in the traditional sintering process.

2. Experimental procedure

Polymeric solutions with ions of interest (Sn, Zn, and Nb) were prepared by Pechini method, comprising the formation of a metal ion complex, followed by the addition of a polymerizing agent. The polymeric precursor method involves the immobilization of the complex in the organic matrix, thereby substantially reducing the segregation of metals during the decomposition of the polymer at high temperatures, ensuring a homogeneous composition.[22,23]

Table 1
Raw materials used in the synthesis (analytical purity – PA).

Reagents	Provider
$SnCl_2{\cdot}2H_2O$, $C_2H_6O_2$ (ethyleneglycol), HF	Synth
ZnO	Unimauá
Nb_2O_5	CBMM
$C_6H_8O_7$ (citric acid), $AgNO_3$, $CaCO_3$	Merck
HNO_3, NH_4OH	Quemis

The raw materials used in this work are shown in Table 1. All initial materials were of analytical purity (PA). First, the tin chloride was dissolved in aqueous HNO_3 solution and by addition of NH_4OH took place the precipitation until the solution showed pH ≈ 8 when was obtained $Sn(OH)_2$. The Cl^- elimination was performed by washing precipitate of $Sn(OH)_2$ with distilled water that was checked by test with $AgNO_3$. $Sn(OH)_2$(s) was mixed with aqueous citric acid solution and then ethylene glycol was added; molar ratio was 1:3:6 (metal:citric acid:ethylene glycol). The preparation of zinc oxide solution was similar to previous one: dissolution in aqueous HNO_3 solution, precipitation with NH_4(OH) (until the solution showed pH ≈ 8) and mixing the precipitate obtained with citric acid and ethylene glycol in the molar ratio of 1:4:16. The niobium oxide was dissolved in HF and precipitated with NH_4(OH) until the solution showed pH ≈ 8 (washing the precipitate with distilled water to give a negative test for fluoride ions using $CaCO_3$). The niobium hydroxide obtained was dissolved in aqueous citric acid solution with subsequent addition of ethylene glycol, also in a molar ratio of 1:4:16.

The ceramic powders are obtained by mixing (98.95 mol% SnO_2, 1.00 mol% ZnO and 0.05 mol% Nb_2O_5) and controlled calcination of the resin (500 °C/2 h) until the full formation of the oxides, which was followed by milling to obtain particles of uniform and nanometric size. The characterization of SnO_2-based powder by XRD, BET and SEM was carried out. XRD measurements were obtained by Rigaku equipment RINT2000 model, considering the experimental condition: range of 20–80° with $\Delta 2\theta = 0.02°$ by increment and copper radiation, 40 kV, 20 mA. The XRD patterns of the samples were analyzed and compared with JCPDS-ICDD card. The BET method, used to obtain information about the surface area of the samples is based on studies of adsorption-desorption of N_2 gas in the samples, were carried out by ASAP 2010 equipment. The SEM images were obtained by JEOL 7500F model-field emission scanning electron microscope, thus making a qualitative morphological analysis of grains and pores of the prepared samples.

To achieve the smaller size and weight, which facilitates the integration to integrated circuit technology system, the samples were prepared in the film form. For this purpose, the electrophoretic deposition (EPD) was used for the ceramic film deposition by applying a tension in a stable ethylic suspension of SnO_2 nanoparticles. This method has been used since it ensures a uniform and fast deposition.[24–26] The system

consists of a pair of electrodes (positive and negative poles) and the electrolytic cell constituted by a small glass container, where the electrodes, substrate and the suspension of the particles are placed.

The substrate used for the deposition of particles (Si(1 0 0)/TiO_2 (1 μm)/Ti (20 nm)/Pt (150 nm) was fixed to the negative electrode and immersed in alcoholic suspension composed of particles of SnO_2 (20 mL ethanol with 7 mg of powder). The electrode of the system were modified by magnets to the deposition of particles to enhance the ionization process from the orientation of the dipole alignment of particles thereby increase the deposition rate due to the presence of a magnetic field. NdFeB magnets with Ni surface treatment and 11 mm × 1.5 mm circular shape were used, two magnets were placed behind negative electrode and one magnet is placed behind the positive electrode.

Moreover, it was also added to the suspension 0.02 g of solid iodine to increase the charge on the surface of the particles and enhance the deposition of these on the substrate. It was used for depositing a high-voltage source Hipot ET 5000 cc Serta, a voltage of 2 kV was applied for 10 min. After deposition of SnO_2-based particles on the substrate, the obtained film was exposed to a heat treatment at 250 °C/30 min arranged to remove iodine.

The sintering process was carried out at 1000 °C/40 min in a CEM-Phoenix microwave oven with magnetron of 770 W and frequency of 2.45 GHz, adapted by the research group itself in our laboratory to reach high temperatures. It is worthy pointing out that microwave oven was used owing to the fact that it presents a faster and homogeneous sintering at a lower temperature compared to a conventional one, thus it aids in decreasing the costs of preparing the material. The microwave energy generates heat inside the particles by interaction atoms-electromagnetic field, thereby allowing the volumetric heating of the material through formation of temperature gradients and heat flow from inside to the outside of the material. The sintering occurs due to the action of two mechanisms that optimize the diffusion of material and densifies more easily compared to normal heating and can happen simultaneously or in an isolated way, namely: electric dipole rotation (ionic conduction) and the phenomenon induction. By using microwave oven is possible to observe the decrease of the sintering temperature and time to achieve a predetermined density and also decrease the segregation of ions or the formation of secondary phases at grain boundaries.[27,28]

The layer of Cr^{3+} was deposited by electrophoresis under the same conditions for all samples: the sintered film has been placed on the negative electrode and immersed in a cell containing Cr^{3+} ionic solution (0.3 mol L^{-1}) and then was applying a voltage of 2 kV for 5 min. Finally, each film was thermally treated in a microwave oven to promote the diffusion of Cr^{3+} in the film through the grain boundary. The electrical characterization of current vs. voltage (I vs. V) was carried out. A study of electrical properties was performed using the sample previously heat treatment at 900 °C and 1000 °C for 5, 10 and 15 min to promote Cr^{3+} diffusion in the films. Eq. (7), derived from Eq. (4), was used to evaluate the nonlinear coefficient of curves. The calculation of α relative to the electric field (E) and current density (J) is defined in Eqs. (5) and (6).[28,29]

$$\alpha = \frac{\log\ J_2 - \log J_1}{E_2 - E_1} \tag{4}$$

Values of the electric field and current density are obtained from the equations:

$$E = \frac{V}{d} \tag{5}$$

$$J = \frac{I}{A} \tag{6}$$

where d represents the sample thickness and A the area of the electrode deposited on the surface of the film. For the calculation of α, we use the range of 1–10 mA/cm^2 current density, i.e., $J_1 = 1$ and $J_2 = 10$, then:

$$\alpha = (\log\ E_2 - \log E_1)^{-1} \tag{7}$$

For electrical characterization the platinum top electrodes were deposited on surface using a circular mask with holes through RF Sputtering technical. Impedance spectroscopy measurements using the frequency range of 10 Hz to 1 MHz (Autolab) were obtained in order to evaluate the effect of Cr^{3+} diffusion. The impedance measurements were taken at room temperature with an amplitude voltage of 0.5 V. For impedance spectroscopy measurements used a variable frequency sinusoidal supply and the detected current was used as an answer.

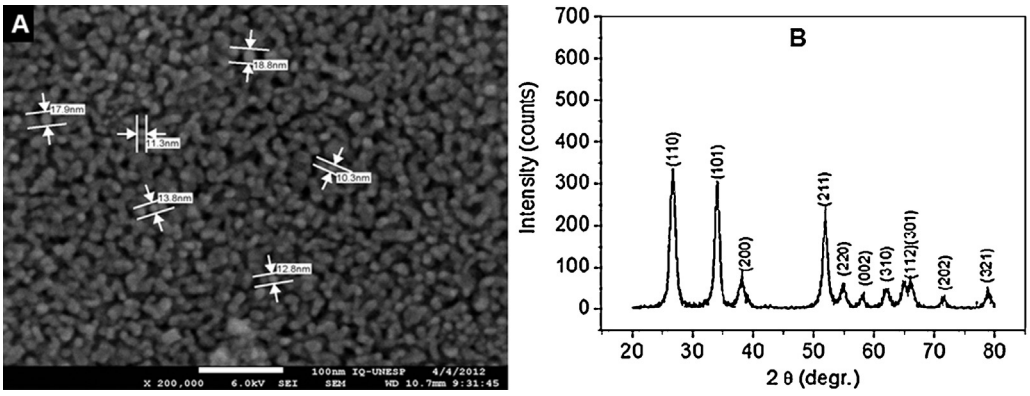

Fig. 1. (a) SEM images and (b) XRD of SnO_2·Nb_2O_5·ZnO-powder after calcination at 500 °C/2 h of polyester resin followed by milling.

The analysis of the graphs obtained by impedance spectroscopy provides information such as the resistance of the sample. The high frequency semicircles are related to the resistivity presented by the grain.[11,30,31]

3. Results and discussion

The polymeric solution composed of SnO_2 with 1 mol% of ZnO and 0.05 mol% of Nb_2O_5 was calcined in a muffle furnace. The powder obtained was milled in the Atritor mill using ethanol as median. After milling the specific surface area (BET) is 57 m^2/g.

Fig. 1b shows the X-ray diffraction pattern for the $SnO_2{\cdot}ZnO{\cdot}Nb_2O_5$ powder calcined and milled, the peaks observed are attributed to the crystalline phase of the SnO_2 rutile (JCDPS No. 41-1445) showing no evidence of any secondary phases. The same powder was analyzed by scanning electron microscopy (SEM) and presented in Fig. 1a. As observed, the particles are spherical with uniform distribution of size and average diameter of 15 nm.

The powder illustrated in Fig. 1 was fractionated to select particles of average diameter size of about 10 nm in this procedure. The $SnO_2{\cdot}Nb_2O_5{\cdot}ZnO$-powder was put in ethanol and the suspension placed on a column of 50 cm height and 3 cm diameter. This will allow separate two fractions, agglomerated particles and particles dispersed through gravimetric separation. The solution has been placed in the column for 20 min, the volume in the lower half of the column (containing agglomerated particles) was separated from the volume in the upper half of the column containing the smaller and dispersed particles. The amount collected from the upper half of the column was subsequently used for the preparation of the films by EPD. For sintering of the films, after carrying out a few tests in a microwave oven to evaluate the thickness and sintering of the particles, the best conditions were reached at 1000 °C for 40 min, according to the operating limit of the oven. The results of the SEM analysis for the sintered SnO_2-based film are shown in Fig. 2. It is possible to observe a homogeneous film with a thickness of 5 μm with presence of pores and the formation of necks between the particles. All observed films have the same characteristics.

It is known that the thickness of the film obtained by the EPD technique can be controlled by the deposition time, optimizing the breakdown voltage which depends on the number of potential barriers (grain size) and barrier voltage (constant in this case) according to Eqs. (8) and (9).

$$N_b = \frac{t}{d} \tag{8}$$

$$V_b = \frac{E_b}{N_b} \tag{9}$$

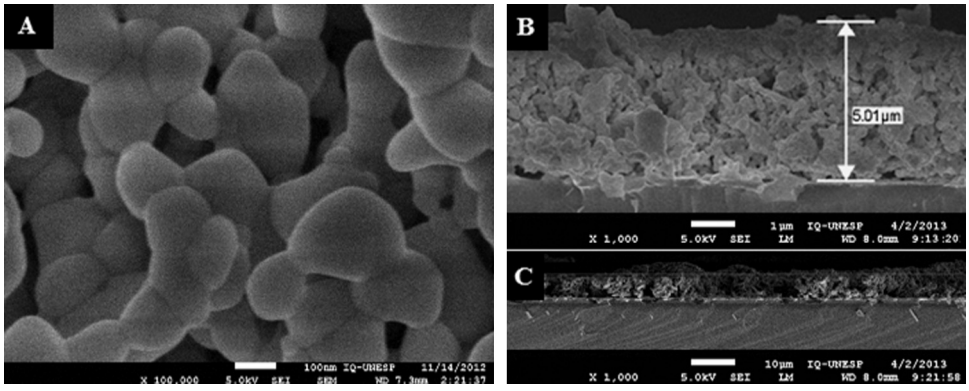

Fig. 2. SEM of the film deposited by electrophoresis and sintered at 1000 °C/40 min: (a) top vision; (b) and (c) different magnifications of cross section vision.

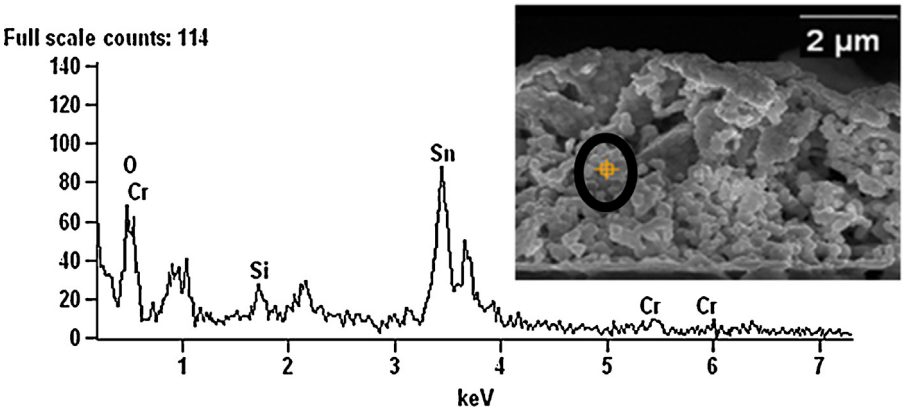

Fig. 3. EDS image of film after deposition of Cr^{3+} by EPD technique and heat treatment at 1000 °C/15 min.

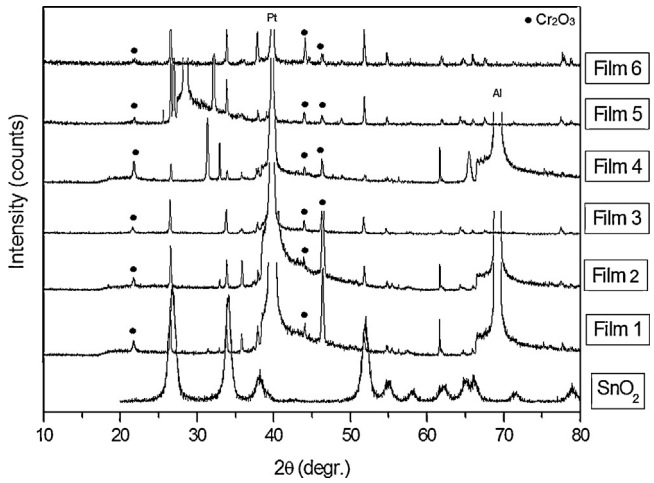

Fig. 4. XRD analysis of SnO_2-based powder and of SnO_2-based films after heat treatment at microwave oven for diffusion of Cr^{3+}.

where the number of effective barriers is denoted by N_b, fixed thickness of the sample (t), grain sizes (d), the voltage per barrier at grain boundary (V_b), and E_b is the breakdown electrical field.

The results obtained by EPD for films immersed in the cell with 0.3 mol L^{-1} of chromium ions solution, indicate that the deposition of Cr^{3+} ions on the sintered films surface occurred and from the EDS analysis in Fig. 3 (area highlighted) it can be noticed that the deposition of chromium ions was effective along the film's thickness and showed no evident indication of presence of contaminant metals.

Following Cr^{3+} deposition, each film was thermally treated in a microwave oven to promote the diffusion of these ions along the film for modification of grain boundary region. The first sample, noted as Film 0, the chromium was not deposited to compare the influence of Cr^{3+} on the electrical properties. Afterwards the thermally treatment the films were characterized by XDR (Fig. 4) to verify secondary phase formation or segregation on grain boundary. Also, was characterized using voltage vs. current analysis (Fig. 5) as well as impedance spectroscopy (Fig. 6) to assess the electrical properties regarding the diffusion of chromium.

In the X-ray diffraction pattern, Fig. 4, low intensity peaks outside the SnO_2 spectrum are observed and were identified as belonging according JCPDS data chromium oxide which crystallized in grain boundaries after the heat treatment. Also, some high intensity peaks present in the XRD patterns of the films were assigned to substrate (Pt) and sample holder (Al). In turn the peaks relating to the SnO_2 no changes such as shift in value of 2 theta or splitting peaks, this indicates that chromium is present mostly as the secondary phase Cr_2O_3 located in the grain boundary. Results of varistor properties were improved by the presence of the chromium rich phase. That confirms previous results which indicate the action of Cr_2O_3 is in the grain boundary region, influencing the formation of the potential barrier as observed in electrical properties illustrated in Fig. 5 and Table 2.

The nonlinear coefficient (α), breakdown voltage (V_R) and leakage current (I_F) were calculated for all films and are presented in Table 2. The breakdown voltage is obtained when the varistor begins to show the electrical conductivity, which value is determined as the value of applied voltage related to the current density equal to 1 mA/cm^2. The leakage current was determined as the value of the current when the voltage reached 70% of the breakdown voltage. The term I_F represents the current passing through the material before it reaches the breakdown voltage. Table 2 shows the data obtained from the curves in Fig. 5.

The Film 5 and Film 6 showed better varistor behavior. To verify the efficiency of the used technique on the reproducibility of electrical properties, another samples were prepared and thermally treated at 1000 °C for 10 min (Film 5.1 and Film 5.2) and for 15 min (Film 6.1 and Film 6.2). The values of the varistor parameters for these new samples are presented in Table 3.

Analyzing the curves J vs. E, Fig. 5, and the calculated values for α, E_R and I_F in Tables 2 and 3, it can be concluded that film without Cr^{3+} presented much lower values when compared to the films that were modified with chromium. It is also possible to observe that promoting the diffusion of Cr^{3+} ions with increasing of heat treatment leads to a significant change in the electrical properties. It can be inferred that the addition of chromium promote modification in the potential barrier in the grain boundary region with improvement in the values obtained of α (from 1.7 to over 10) and E_R (from 2.5 to over 50 V) and a decrease in the values of I_F (from 10^{-4} to less than 10^{-6} A). This behavior can well be explained owing to the defects created by the additives that are responsible for the modification of Schottky-type

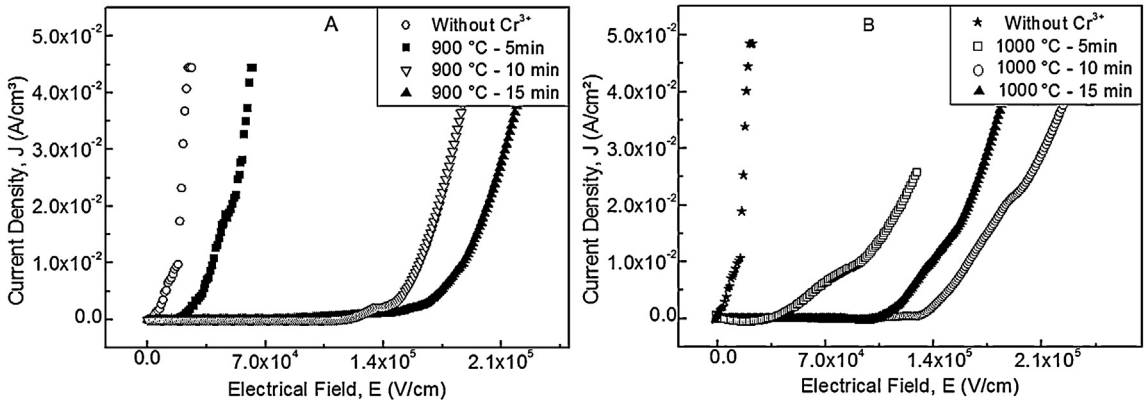

Fig. 5. Graphs of current density vs. electric field: (a) for films without Cr^{3+} and films thermally treated at 900 °C and (b) films thermally treated at 1000 °C after the Cr^{3+} deposition.

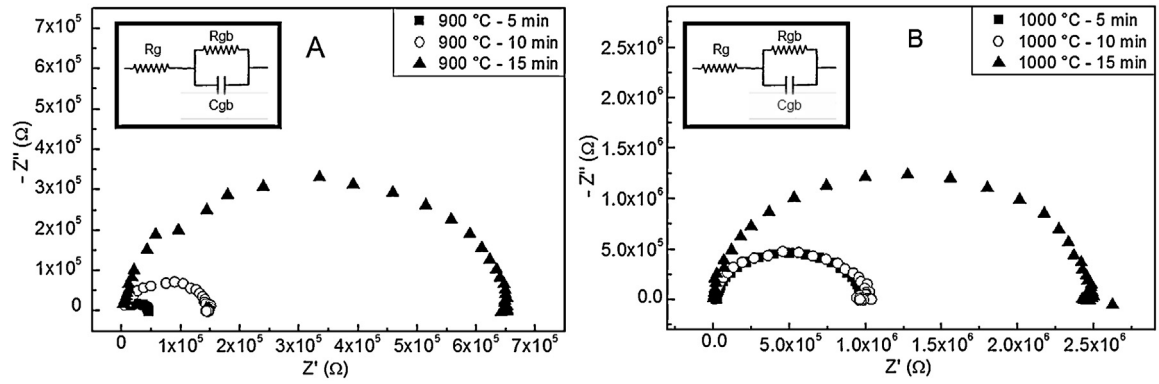

Fig. 6. Nyquist diagram: (a) for films thermally treated at 900 °C after Cr^{3+} deposition and (b) for films thermally treated at 1000 °C after the deposition of Cr^{3+}.

Table 2
Values calculated for the coefficient of nonlinearity (α), breakdown electric field (E_R), breakdown voltage (V_R) and leakage current (I_F).

Sample	Heat treatment (°C/min)	α	E_R (kV/cm)	V_R (V)	I_F (A)
Film 0	(Without Cr^{3+})	1.7	5.0	2.5	6.8×10^{-4}
Film 1	900/5	4.2	22.0	11.0	5.4×10^{-4}
Film 2	900/10	5.8	128.0	64.0	6.7×10^{-4}
Film 3	900/15	7.2	130.0	65.0	2.8×10^{-4}
Film 4	1000/5	9.6	48.0	24.0	4.6×10^{-4}
Film 5	1000/10	10.3	125.0	62.5	4.4×10^{-5}
Film 6	1000/15	11.4	119.0	59.5	4.8×10^{-6}

Table 3
Values calculated for the coefficient of nonlinearity (α), breakdown electric field (E_R), breakdown voltage (V_R) and leakage current (I_F).

Sample	Heat treatment (°C/min)	α	E_R (kV/cm)	V_R (V)	I_F (A)
Film 5.1	1000/10	10.5	141.0	70.4	6.2×10^{-6}
Film 5.2	1000/10	10.8	157.0	78.5	1.6×10^{-6}
Film 6.1	1000/15	13.8	151.0	75.5	8.5×10^{-6}
Film 6.2	1000/15	11.5	120.0	60.4	2.8×10^{-6}

potential barriers in the grain boundaries. The data presented in Table 3 revealed a reproducibility of electrical properties according to the process used to prepare the samples. Further study to I vs. V parameters as a function of temperature will be carried out willing to determine the conductivity (resistivity) and the parameters of the potential barrier of the films.

The films were examined by impedance spectroscopy (frequency range of 10 Hz to 1 MHz). The equivalent circuit model for varistor ceramics is composed of two series circuits of a resistance and capacitor in parallel, thus, the electrical response can be modeled.[32]

The Nyquist diagram is composed of only a semicircle, as shown in Fig. 6, in this way, it is not possible to identify the specific contributions of grain, grain boundary and electrode on the total resistance of the samples. The equivalent circuit model was inserted in the graphs showing the grain resistance (R_g) in series with the resistance of the grain boundary (R_{gb}) and capacitance (C_{gc}) in parallel.

With the data collected from the impedance analysis, it was possible to verify the grain resistance (ρ_g). The value R_g (Ω cm) of the films is calculated using Eq. (10) [33]:

$$R_g = R\left(\frac{S}{l}\right) \quad (10)$$

Table 4
Values calculated for resistance of the samples after Cr^{3+} deposition.

Sample	Heat treatment (°C/min)	R (kΩ)	ρ_G (kΩ cm)
Film 1	900/5	44.0	19.8
Film 2	900/10	149.5	67.3
Film 3	900/15	651.5	293.1
Film 4	1000/5	988.6	444.9
Film 5	1000/10	994.4	447.5
Film 6	1000/15	2622.2	1180.1

where R is the resistance (Ω) obtained from the diameter of the semicircle of high-frequency, S (cm^2) is the electrode area and l (cm) is thickness of the sample.

Table 4 shows the values of film resistance (R) and grain resistance (R_g). The Film 1 possesses very low values compared to the other films, which could indicate the smaller diffusion of Cr^{3+}. The higher value at Film 6 probably indicates that the Cr^{3+} has influence on the crystal structure. Meanwhile, further more detailed study may be needful to support this assumption. It is obviously note that the processing parameters have strong influence onto the total resistance of the material. The time duration and annealing temperature lead to an increase of electrical resistance for the varistor films. The films exposed to shorter time

and lower temperature show a much lower resistance compared to the other films. This conclusion confirms the result obtained for the Film 6 (longest time and higher temperature of thermal treatment), which shows a highest resistance.

4. Conclusions

SnO_2-based powder was synthesized by Pechini method. The EPD allowed obtaining films with homogeneous thickness and was effective for deposition of chromium ions on films surface, also. The microwave oven was effective to provide sintering and diffusion of chromium.

The nonlinearity coefficient was increased from 1.7 (film without Cr^{3+} deposition) to 11.4 when the sample was treated to 1000 °C/15 min following the deposition of Cr^{3+}. The breakdown voltage for all films was less than 80 V.

It was clear the improvement of varistor behavior of the films after Cr^{3+} deposition and thermally treatment, indicating the Cr^{3+} influence on electrical properties.

Acknowledgements

The authors thanks to the LMA-IQ for providing the FEG-SEM facilities, and the financial support of this research project by the Brazilian research funding agencies CNPq and CEPID/CDMF-FAPESP 2013/07296-2.

References

1. Matsuoka M. Non-ohmic properties of zinc-oxide ceramics. *Jpn J Appl Phys* 1971;**10**:736–46.
2. Aguilar-Martínez JA, Pech-Canul MI, Hernándes MB, Glot AB, Rodríguez E, Ortiz LG. Effect of sintering temperature on the electric properties and microstructure on SnO_2–Co_3O_4–Sb_2O_5–Cr_2O_3 varistor ceramic. *Ceram Int* 2013;**39**:4407–12.
3. Lu ZY, Glot AB, Ivon AI, Zhou ZY. Electrical properties of new tin dioxide varistor ceramics at high currents. *J Eur Ceram Soc* 2012;**32**:3801–7.
4. Brankovic G, Branlovic Z, Varela JA. Nonlinear properties and stability of SnO_2 varistor prepared by evaporation and decomposition of suspensions. *J Eur Ceram Soc* 2005;**25**:3011–5.
5. Santos PA, Maruchin S, Menegoto GF, Sara AJ, Pianaro AS. The sintering time influence on the electrical and microstructural characteristics of SnO_2 varistor. *Mater Lett* 2006;**60**:1554–7.
6. Mazloom J, Ghodsi FE. Spectroscopic, microscopic and electrical characterization of nanostructured SnO_2:Co thin films prepared by sol–gel spin coating technique. *Mater Res Bull* 2013;**48**:1468–76.
7. Lee HJ, Kim CD, Kang S, Kim IW. Nonlinear *I–V* characteristics of Ta_2O_5-, Nb_2O_5-, V_2O_5-doped SnO_2 based varistor ceramics. *J Korean Phys Soc* 2007;**51**:594–8.
8. Metz R, Koumeir D, Morel J, Pansiot J, Houabes M, Hassanzadeh M. Electrical barriers formation at the grain boundaries of Co-doped SnO_2 varistor ceramics. *J Eur Ceram Soc* 2008;**28**:829–35.
9. Cilense M, Ramirez MA, Foschini CR, Leite DR, Simões AZ, Bassi W, et al. Effect of seed addition on SnO_2-based varistors for low voltage application. *J Am Ceram Soc* 2013;**96**:524–30.
10. Moura Filho F, Simões AZ, Ries A, Perazolli L, Longo E, Varela JA. Nonlinear electrical behavior of the Cr_2O_3, ZnO, CoO and Ta_2O_5-doped SnO_2 varistor. *Ceram Int* 2006;**32**:283–9.
11. Wang CM, Wang JF, Wang CL, Chen HC, Su W, Zang GZ, et al. Nonlinear electrical characteristics of SnO_2·CuO ceramics with different donors. *J App Phys* 2005;**97**, 126103-1–126103-3.
12. Gasparotto G, Perazolli L, Jacomaci N, Ruiz M, Zaghete MA, Foschini CR, et al. SnO_2 dense ceramic microwave sintered with low resistivity. *Mater Sci Appl* 2012;**3**:272–80.
13. Bacelar WK, Bueno PR, Leite ER, Longo E, Varela JA. How Cr_2O_3 influences the microstructure and nonohmic features of the $SnO_2(Co_x, Mn_{1-x})O$-based varistor system. *J Eur Ceram Soc* 2006;**26**:1221–9.
14. Daghe SR, Ravi V, Yang OB. Varistor property of SnO_2·CoO, Ta_2O_5 ceramic modified by barium and strontium. *J Alloy Compd* 2008;**466**:483–7.
15. Glot AB, Gaponov AV, Sandoval-García AP. Electrical conduction in SnO_2 varistors. *Physica B* 2010;**405**:705–11.
16. Wang YJ, Wang JF, Li CP, Chen HC, Su WB, Zhong WL, et al. Effects of niobium dopant on the electrical properties of SnO_2-based varistor system. *J Mater Sci Lett* 2001;**20**:19–21.
17. Hu G, Zhu J, Yang H, Wang F. Effect of Cr_2O_3 addition on the microstructure and electrical properties of SnO_2-based varistor. *J Mater Sci: Mater Electron* 2013;**24**:1735–40.
18. Filho FM, Simões AZ, Ries A, Perazolli L, Longo E, Varela JA. Dependence of the nonlinear electrical behavior of SnO_2-based varistors on Cr_2O_3 addition. *Ceram Int* 2007;**33**:187–92.
19. Wang WX, Wang JF, Chen HC, Su WB, Zang GZ. Effects of $C_{r2}O_3$ on the properties of (Co, Nb)-doped SnO_2 varistors. *Mat Sci Eng B* 2003;**99**:470–4.
20. Aguilar-Martinez JA, Pech-Canul MI, Hernandez MB, Glot AB, Rodriguez E, Garcia Ortiz L. Effect of Cr_2O_3 on the microstructure and non-ohmic properties of (Co, Sb)-doped SnO_2 varistors. *Rev Mex Fis* 2013;**59**:6–9.
21. Cássia-Santos MR, Sousa VC, Oliveira MM, Bueno PR, Bacelar WK, Orlandi MO, et al. Cerâmicas eletrônicas à base de SnO_2 e TiO_2. *Cerâmica* 2001;**47**:136–43.
22. Pechini MP. Method of preparing lead and alkaline titanates and niobates and coating method using the same to form a capacitor; 1967. U.S. Patent n. 3330697.
23. Stojanivic BD, Foschini CR, Cilense M, Zaghete MA, Cavalheiro AA, Paiva-Santos CO, et al. Structural characterization of organometallic-derived 9.5/65/35 PLZT ceramics. *Mater Chem Phys* 2001;**68**:136–41.
24. Gurrappa I, Binder L. Electrodeposition of nanostructured coatings and their characterization – a review. *Sci Technol Adv Mater* 2008;**9**:043001–12.
25. Corni I, Ryan MP, Boccaccini AE. Electrophoretic deposition: from traditional ceramics to nanotechnology. *J Eur Ceram Soc* 2008;**28**:1353–67.
26. Choi WB, Jin YW, Kim HY, Lee SJ, Yun MJ, Kang JH, et al. Electrophoresis deposition of carbon nanotubes for triode-type field emission display. *App Phys Lett* 2001;**78**:1547–9.
27. Perazolli LA, Gasparotto G, Jaomaci N, Ruiz M, Zaghete MA, Foschini CR, et al. SnO_2 dense ceramic microwave sintered with low resistivity. *Mater Sci Appl* 2012;**3**:272–80.
28. Gasparotto G, Bordignon MAN, Foschini CR, Gasparotto G, Aguiar EC, Zaghete MA, et al. SnO_2 ceramics with low electrical resistivity obtained by microwave sintering. *J Adv Microsc Res* 2011;**6**:1–8.
29. He J, Peng Z, Fu Z, Wang Z, Fu X. Effect of ZnO doping on microstructural and electrical properties of SnO_2–Ta_2O_5 based varistor. *J Alloy Compd* 2012;**528**:79–83.
30. Metz R, Koumeir D, Morel J, Pansiot J, Houabes M, Hassanzadeh M. Electrical barriers formation at the grain boundaries of Co-doped SnO_2 varistor ceramics. *J Eur Ceram Soc* 2008;**28**:829–35.
31. Tadokoro SK, Muccillo ENS. Tetragonal zircônia polycrystals. Part II: Microstructure and electrical resistivity. *Cerâmica* 2001;**47**:100–8.
32. Lu ZY, Glot AB, Ivon AI, Zhou ZY. Electrical properties of new tin dioxide varistors ceramics at high currents. *J Eur Ceram Soc* 2012;**32**:3801–7.
33. Zang GZ, Li LB, Liu HH, Wang XF, Gai ZG. Impedance performances of SnO_2–Zn_2SnO_4 composite ceramics. *J Alloy Compd* 2013;**580**:611–3.